Environmental Science Nano

ROYAL SOCIETY OF CHEMISTRY

PAPER

View Article Online
View Journal | View Issue

Check for updates

Cite this: *Environ. Sci.: Nano*, 2021, **8**, 666

Enrichment of uranium from wastewater with nanoscale zero-valent iron (nZVI)†

Yilong Hua,[ab] Wei Wang,[b] Nan Hu,[a] Tianhang Gu,[b] Lan Ling[b] and Wei-xian Zhang*[b]

Received 15th October 2020,
Accepted 14th January 2021

DOI: 10.1039/d0en01029d

rsc.li/es-nano

The core–shell structure of nanoscale zero-valent iron (nZVI) offers multiplex solution and surface chemistry for reliable and high-efficiency enrichment and separation of uranium from low-level sources such as wastewater, groundwater, and even seawater. In this work, the reduction, enrichment and separation of uranium from uranium-tailings wastewater were demonstrated in continuous-flow reactors. Specifically, a two-stage continuous flow stirred tank reactor system was operated for 193 h. 497.7 L of radioactive uranium-tailings wastewater containing ~331 μg U per L was treated with a total of 60.22 g of iron nanoparticles. It produced reacted nZVI containing ~0.19 wt% uranium, well above typical high-grade uranium ores. The treated wastewater had an average concentration of just 1.47 μg U per L. High-resolution elemental mappings performed with aberration corrected scanning transmission electron microscopy (Cs-STEM) indicated that uranium was deposited largely in the core area of the reacted nZVI particles with chemical reduction as the principal enrichment mechanism. Together with our previous work on nZVI, this further offers growing evidence of a cost-effective nanotechnology for simultaneous pollution control and resource recovery.

Environmental significance

Nanoscale zero-valent iron (nZVI) offers rich solution and surface chemistry for reliable and high-efficiency enrichment and separation of uranium from low-level sources such as wastewater, groundwater, and even seawater. In this work, the reduction, enrichment and separation of uranium from uranium-tailings wastewater were demonstrated in continuous-flow reactors. Data presented in this work provide further proof of a cost-effective nanotechnology for simultaneous pollution control and resource recovery.

1. Introduction

Recent research demonstrated that uranium can be separated quickly and completely from wastewater with nanoscale zero-valent iron (nZVI).[1–5] The dissolved uranium can be quickly reduced to U(v)/U(iv) and deposited in the core area of the core–shell nanostructure. This reaction was captured with aberration corrected scanning transmission electron microscopy (Cs-STEM), which produced high-resolution elemental mappings of Fe, O and U in a single nZVI nanoparticle. Experimental data showed that even with trace U(vi) in the wastewater (*e.g.*, ≪1 ppm), uranium accumulated in the reacted nZVI can reach g kg^{-1} level (>0.1% wt) in the solids.[1] This points to a potential mechanism for high-efficiency uranium recovery and pollution control.

In this research, the above theoretical understanding is further verified with uranium tailings wastewater treated in continuous-flow reactors commonly used in wastewater treatment. Uranium tailings wastewater contains high concentrations of toxic but valuable uranium, as well as many other heavy metal and metalloid contaminants (*e.g.*, As, Cd, Ni, and Se).[6] Intentional and accidental discharge or leakage of uranium-containing wastewater not only cause serious damage to the environment and threaten human health, but also waste important strategic resources.[7–10] The 2011 Fukushima Daiichi Nuclear Disaster taught the world a somber lesson on the disastrous impact of failed nuclear reactors and the severe lack of effective mitigation and control measures for a supposedly modern and safe technology.[11]

So far, manipulating the chemical solubility and mobility of uranium ions in water remains as the primary approach employed for the mitigation of uranium wastewater. Both

[a] *Key Discipline Laboratory in Uranium Mining and Hydrometallurgy, University of South China, 28 West Changsheng Road, Hengyang, Hunan, 421001, China*
[b] *State Key Laboratory for Pollution Control, School of Environmental Science and Engineering, Tongji University, 1239 Siping Road, Shanghai, 200092, China. E-mail: zhangwx@tongji.edu.cn; Fax: +86 21 65985885; Tel: +86 21 65985885*

† Electronic supplementary information (ESI) available. See DOI: 10.1039/d0en01029d

Published on 20 January 2021. Downloaded by Ege Universitesi on 6/12/2023 6:19:35 PM.

This journal is © The Royal Society of Chemistry 2021

Published on 20 January 2021. Downloaded by Ege Universitesi on 6/12/2023 6:19:35 PM.

abiotic and biotic methods can convert U(VI) to U(V) and/or U(IV). In particular, growing research attention suggests that iron-derived nanomaterials such as nZVI and with various supporting materials (*e.g.*, carbon, diatomite, graphene, illite, Na-bentonite, and carboxymethyl cellulose) have significant potential for uranium treatment and remediation.[5,12–16] Mechanisms for uranium removal may include: (i) adsorption of U(VI) by surface functional groups, (ii) reduction of U(VI) to U(V)/U(IV) by Fe(0) or structural-Fe(II),[17–19] (iii) precipitation of U(VI) in the form of $UO_3{\cdot}2H_2O$,[18] and (iv) encapsulation of uranium in reactive iron nanoparticles.[1] On the other hand, geochemical constituents (*e.g.*, anions, cations, and organic matter) could complex with U(VI) and limit its separation efficiency, compete for the sorption/reduction sites of nZVI, and form non-conductive precipitates on the surface of nZVI and hinder electron transfer for uranium reduction.

Previous laboratory studies have been mostly focused on the kinetics and mechanisms of uranium removal from synthetic uranium-containing solutions and the assessment of the effect of geochemical constituents with the purpose of remediating uranium-contaminated groundwater.[2,4,5,17,19] In this contribution, experiments were conducted to evaluate the performance and dynamics of nZVI in continuous flow reactors and with real-world uranium tailings wastewater containing a relatively high concentration of radioactive uranium, as well as other metal and metalloid contaminants. This is part of our continuous efforts to evaluate the feasibility and scale up of nZVI for large-scale applications in wastewater treatment.

2. Experimental

2.1. Uranium tailings wastewater

The uranium tailings wastewater used in this study was sampled from an active uranium mine in southeastern China. The acidic and strongly oxidative wastewater contained high levels of many metal elements and correspondingly elevated concentrations of anions (Table S1†), including U (averaged at 0.31 ± 0.03 mg L^{-1}), Mn (30.81 ± 1.95 mg L^{-1}) and Ni (2.38 ± 0.45 mg L^{-1}), as well as Mo, Cd, Cr, Co and Se. The uranium concentration was at least two orders of magnitude higher than that of seawater (3.34 μg L^{-1}) and similar to the typical range from 0.84 mg L^{-1} to 2.08 mg L^{-1} of radioactive wastewater.[6,20,21] There were also high-levels of carbonate (565.70 ± 5.24 mg L^{-1}), nitrate (80.88 ± 7.00 mg L^{-1}), sulfate (98.59 ± 7.74 mg L^{-1}), phosphate (2.30 ± 0.46 mg L^{-1}), chloride (99.38 ± 6.86 mg L^{-1}) and fluoride (1.65 ± 0.34 mg L^{-1}) (Table S1†).

2.2. Preparation of nanoscale zero-valent iron (nZVI)

Fresh nZVI was synthesized by the reduction of ferric chloride ($FeCl_3$) with sodium borohydride ($NaBH_4$) according to the method described previously.[22] The sizes of nZVI were in the range of 20–100 nm and average surface area was 34.45 m^2 g^{-1}. The as-prepared nanoparticles were collected by vacuum filtration and stored in ethanol (>99.7%, 4 °C) prior to use.[23–25]

2.3. Continuous flow stirred tank reactors (CSTRs)

The uranium enrichment experiments were performed with two completely mixed reactors in sequence (Fig. 1). One set of experiments was conducted to investigate the effects of reactor operational parameters (*e.g.*, nZVI dose, hydraulic retention time (HRT), and recirculation ratio (*R*)) on uranium enrichment and separation of contaminants while a parallel second set was operated for long-term performance assessment.

Each stage of the nZVI reactors consisted of a reactor (2.58 L) and a sedimentation/nZVI separation tank (2.58 L) made of transparent plastics (polyethylene). Before the wastewater was fed into the nZVI reactor, a predetermined dose of nZVI was added into the reactor, mechanically stirred and recirculated for 20 min till the pH and E_h values of the nZVI slurry reached steady states. Influent wastewater or effluent from the first separation tank was pumped to the first or second nZVI reaction unit to separate contaminants and enrich uranium. The settled nZVI was cycled back to the nZVI reactors or recovered as valuable by-products. High-purity nitrogen gas (>99.999%) was purged into the nZVI reactor to exclude dissolved oxygen throughout the entire experiment. The pH and E_h values of the nZVI slurry were monitored continuously with an Ag/AgCl electrode.

2.4. Chemicals analysis

At predetermined time intervals, samples were withdrawn from the influent and effluent of the reactors. The aqueous samples were filtrated through 0.22 μm PTFE syringe filters, and nZVI slurry was separated by centrifugation and dried in a desiccator under low vacuum (0.1 MPa, 40 °C) for 48 h. All the pretreated samples were digested with concentrated HNO_3 (2%, v/v) and then analyzed. Concentrations of uranium and the metal/metalloid ions were analyzed by inductively coupled plasma mass spectrometry (ICP-MS, Agilent 7700). The measured values were used to determine the aqueous and total concentrations of uranium and other impurities in the solution or their contents in the reacted nZVI solids. Concentrations of bicarbonate was analyzed through volumetric titration, and other anions (F^-, Cl^-, NO_3^-, SO_4^{2-} and PO_4^{3-}) were analyzed by ion chromatography (ICS-5000). A separation factor (K_d) was used to quantify uranium and other metal/metalloid ion sequestration by nZVI:[26]

$$K_d = C_{solids(mmol\ kg^{-1})}/C_{aqueous(mmol\ kg^{-1})} \quad (1)$$

where $C_{solids(mmol\ kg^{-1})}$ and $C_{aqueous(mmol\ kg^{-1})}$ are the concentration of metal/metalloid ions in the reacted nZVI or aqueous solutions.

2.5. Solids analysis

Reacted nZVI particles were harvested for surface morphology and crystallinity analyses. The solids were prepared by depositing a drop of liquid sample on a lacey carbon film supported on a copper grid in a nitrogen-filled glove-box, and its morphological,

Published on 20 January 2021. Downloaded by Ege Universitesi on 6/12/2023 6:19:35 PM.

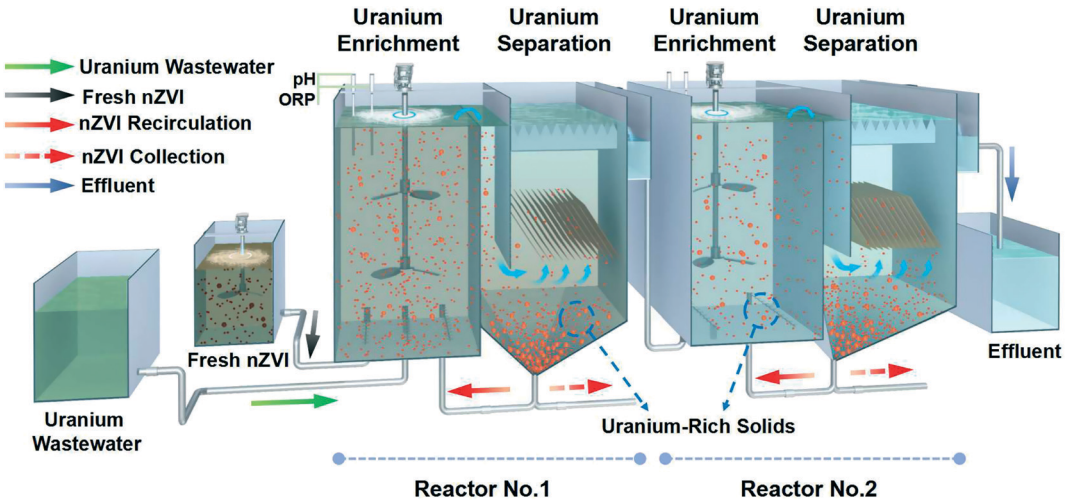


Fig. 1 An illustration of continuous flow stirred tank reactors (CSTRs) for enrichment and separation of uranium from wastewater.

structural and elemental characterization was analyzed using a spherical aberration-corrected scanning transmission electron microscope operated at 200 kV (Cs-STEM, Titan™ G^2 80-200, FEI). The system is equipped with a FEI X-FEG high-brightness Schottky field emission source (brightness 1.8 × 109 A cm^{-2} srad at 200 kV, beam current of 1300 pA in a 0.2 nm spot), a CEOS hexapole-transfer doublet design aberration corrector, a high-angle annular dark-field (HAADF) detector, an energy-filtered TEM (EFTEM, Quantum SE/963 200 kV), and the FEI ChemiSTEM system (SuperX, FEI Co.).[23,27] The HAADF images are often described as the *Z*-contrast (atomic number) imaging since the measured intensity is approximately proportional to the square of the atomic number. STEM-based Energy dispersive X-ray spectroscopy (XEDS) elemental mapping provides unprecedented details as it can capture angstrom resolution distributions of atoms in a nZVI nanoparticle. The STEM-XEDS images provide angstrom resolution elemental mappings of U (Lα), O (Kα) and Fe (Kα) of the nZVI particle. A drift-correction mode was applied during the acquisition of the XEDS maps to minimize the effects of specimen drift.[28]

The solid/surface composition of nZVI was analyzed using an X-ray diffraction instrument (XRD, Bruker D8 Advance). XRD characterization was performed with a Cu Kα radiation source (λ = 1.54178 Å). The operation voltage and tube current were 40 kV and 40 mA. XRD spectra were acquired between 2θ angles from 10° to 90°, with a scanning speed set of 1° min^{-1} and a count time of 0.2 s per step.

A bicarbonate extraction method was used to determine the valence state of uranium on the reacted nZVI particles.[29] Briefly, a 10 mL nZVI slurry was withdrawn from the nZVI reaction unit of CSTR at the end of the experiments and added to a 25 mL bottle with 10 mL bicarbonate solution (0.2 M) which has been purged with high purity nitrogen gas (>99.999%) for 20 min. And then the bottle was sealed and mixed in an end-over-end rotator under anoxic conditions for 1 h. Finally, the suspension was filtered through 0.22 μm PTFE syringe filters and analyzed by ICP-MS.

3. Results and discussion

3.1. Enrichment and separation of U with nZVI in continuous reactors

As shown in Fig. 2, nZVI in a CSTR reactor was efficient for the separation of dissolved uranium from wastewater while the reacted nZVI particles acquired increasingly rich uranium. The average concentration of uranium in the treated effluent was 1.47 μg L^{-1}, far below that in the drinking water standard of USEPA (30 μg L^{-1}) and the targeted treatment breakthrough point of 5 μg L^{-1} (Fig. 2a).

During the experiments, over 99% of uranium was separated from the tailings wastewater (~311 μg U per L) with just 0.12 g nZVI per L. Other metal/metalloid contaminants were also removed (Fig. S1†). Specifically, over 90% of Ni and Cd, and 70–86% of Co, Zn, Cr, Mo, and Se were removed from the wastewater. It was also noted that only 51.18% of Mn was removed by nZVI. The separation factors were 1.30 × 10^6 for U and 1.28 × 10^4–3.53 × 10^5 for other concerned metals (see eqn (1) and Fig. S2†).

After 193 h of continuous operation, 149.94 mg of uranium was recovered from 497.7 L of wastewater with a total of 60.22 g of fresh nZVI added to the reactors in four batches (Fig. 2b). The average concentration of uranium (wt%) in the solids amounted to ~0.19% (Fig. 2b).[30] Furthermore, results from the bicarbonate extraction experiments indicated that most (>82%) of the enriched uranium in the reacted nZVI was in the form of U(IV). The suspension in the nZVI reactors was modest alkaline (pH = 8.5–9.0) and reductive (E_h = −0.10—0.35 V). In fact, these solution conditions favored the U–Fe(0) reactions. Other published works also indicated that reductive and alkaline aqueous conditions are beneficial to uranium separation, especially the reductive immobilization of U(VI) by Fe(0) and/or structural-Fe(II).[2,17,29]

3.2. Aquatic chemistry of fresh nZVI

The outstanding performance of nZVI for enrichment and separation of dissolved uranium is the direct result of the highly

 This journal is © The Royal Society of Chemistry 2021

Published on 20 January 2021. Downloaded by Ege Universitesi on 6/12/2023 6:19:35 PM.

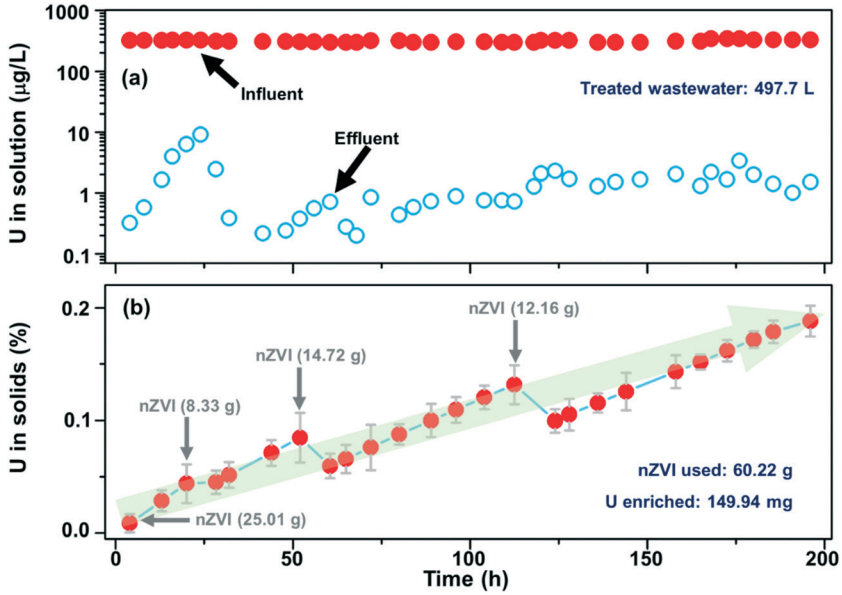


Fig. 2 Treatment and enrichment of uranium from wastewater: (a) concentrations of dissolved uranium in the influent and effluent of the nZVI treatment system; (b) uranium in the reacted nZVI.

favorable solution and surface chemistry of nZVI in water. The core–shell structure of nZVI nanoparticles generates unique surface chemistry for the sorption, reductive transformation and immobilization of dissolved uranium.[1,2] Fig. 3a–d present the STEM-HAADF image and the STEM-XEDS elemental mappings of a typical nZVI particle. The HAADF image shows that the

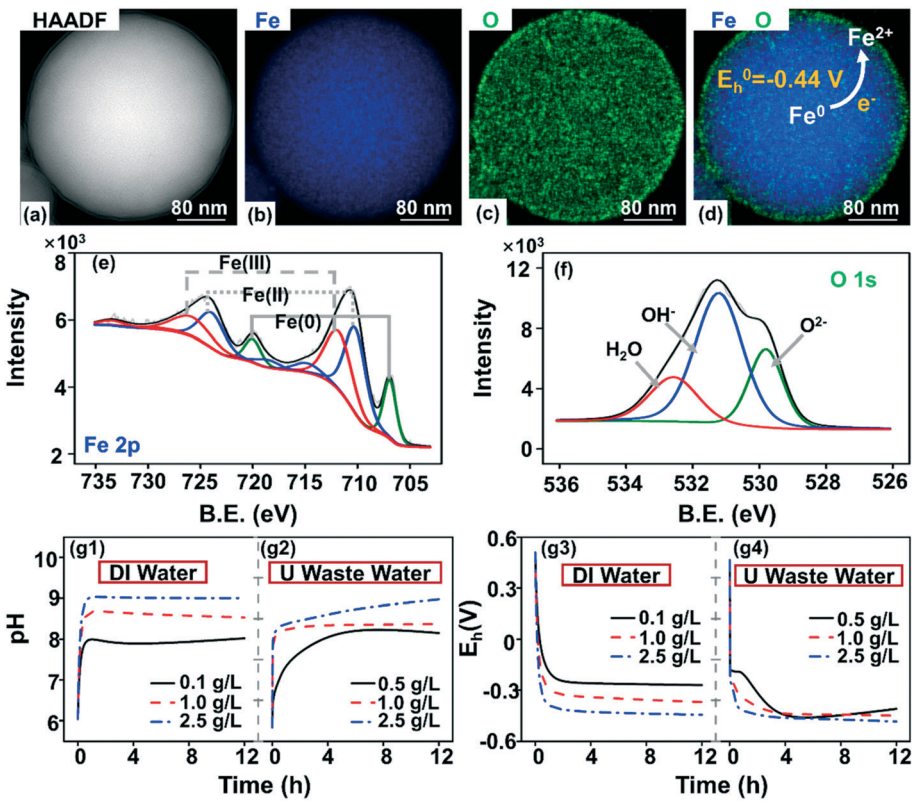


Fig. 3 Characterization of fresh nZVI. (a) HAADF image of a fresh nanoparticle; ((b)–(d)) the elemental mappings of Fe (Kα), O (Kα) and Fe + O overlay, respectively; ((e and f)) XPS spectra of Fe and O; (g) solution pH and E_h trends after nZVI is added into pure water (g1 and g3) and wastewater (g2 and g4).

Published on 20 January 2021. Downloaded by Ege Universitesi on 6/12/2023 6:19:35 PM.

fresh nZVI is spherical with a bright core and distinct shell layer. Elemental mappings (Fe and O) further display the core–shell structure of nZVI that shows a strong signal intensity of Fe in the core, and O is mostly present in the shell layer (Fig. 3b–d).[27]

Curve fitting of the XPS Fe 2p and O 1s spectra revealed the main chemical compositions of nZVI. On the surface, Fe exists as Fe(0), Fe(II) and Fe(III), and O can be in the forms of OH^-, O^{2-} and H_2O (Fig. 3e and f). These results were consistent with the reported nZVI structure in which metallic iron is enclosed with a layer of iron (oxyhydr)oxides.[22,27,31,32] After nZVI particles were added into water, the reactions between the water molecules and metallic iron generated hydroxyl functional groups. Correspondingly, solution pH increased from acidic to alkaline, and solution oxidation–reduction potential decreased from oxidative to strongly reductive within a few minutes (Fig. 3g1–g4). These solution conditions all favor the sorption of metal cations to the negative nZVI surface.

3.3. Uranium in the reacted nZVI

Fig. 4 presents the characterization of the reacted nZVI with Cs-STEM (FEI Titan™ G^2 80-200). In the continuous-flow reactors, nZVI nanoparticles were extensively oxidized with the core–shell structure being transformed from spherical to sheets and needle-like forms (Fig. 4a). The Fe, O and U elemental mapping images suggest that the spherical particles exhibited higher intensity of U and Fe (Fig. 4b–d).

Results of the STEM-XEDS quantification analysis (Fig. 4a and e and Table S2†) indicated that the spherical particles contained >55 wt% Fe and <27 wt% O while the needle-like particle included 33.13 wt% Fe and 49.91 wt% O. The average abundance of U was 0.68 wt% within circle 1 and 0.50 wt% within circle 2 for a reacted nZVI nanoparticle, and only 0.14 wt% in circle 3 of the needle-like aged nZVI (Fig. 4a). For one spherical particle (Fig. 4e), the percentage of U increased from 1.05 wt% to 1.48 wt% within the area of circle 1 to circle 4. And the abundance of Fe increased from 66.66 wt% to 71.73 wt%, while that of O decreased from 3.76 wt% to 2.70 wt% from circle 1 to circle 4. These results indicated that the spherical particle was composed of a dense iron core, and the immobilized uranium accumulated more in the inner zone. The configuration and reactivity of the spherical particle was similar to fresh nZVI. XRD spectra showed that Fe(0), FeO and $MnFe_2O_4$ were the major iron phases within the spent nZVI particles (Fig. S3†).

In short, these experimental results demonstrated that the uranium encapsulation capacity of nZVI was much higher than that of iron (oxyhydr)oxides and the U–nZVI complex was more stable than conventional U sorbed on iron oxides. For example, previous work recorded a uranium removal capacity of 2.40 g g^{-1} for pure nZVI and 8.17 g g^{-1} for nZVI–graphene composites.[1,33] More importantly, uranium is converted to the reduced states (*e.g.*, U(IV)), and primarily deposits in the core area of nZVI.[1,3] In comparison, for lepidocrocite, goethite, hematite, and magnetite, the adsorption capacity is much less than 100 mg g^{-1}.[34–36] Surface adsorbed uranyl could easily be remobilized by the changes in solution pH, ionic strength, and the presence of complexing ligands.

3.4. Assessment of operational parameters

Performance of the nZVI system for uranium separation depends, as expected, on operational conditions such as

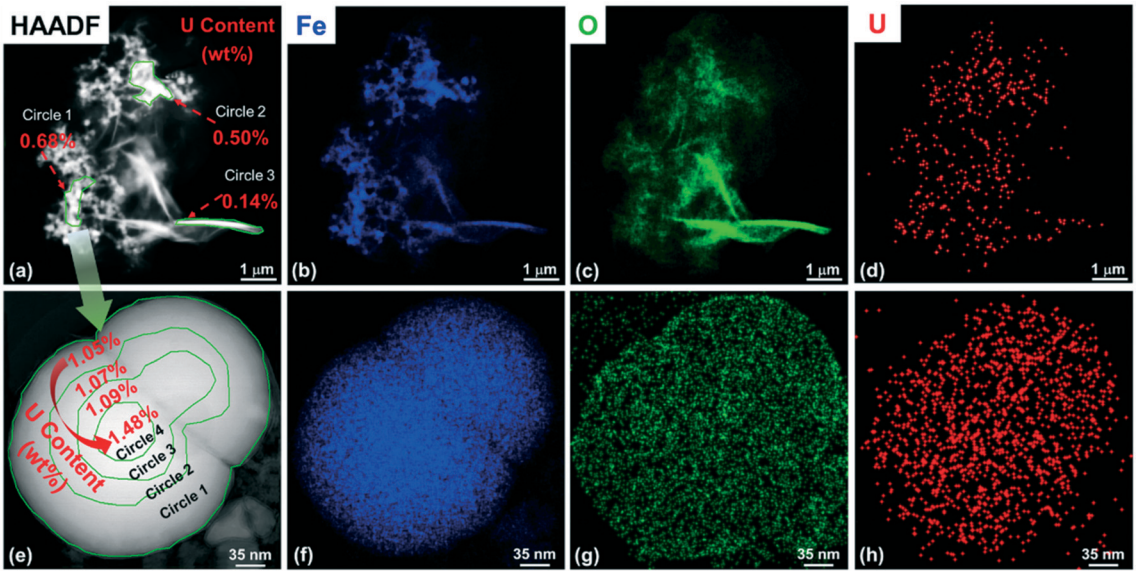


Fig. 4 Characterization of nZVI after reactions with uranium-containing wastewater for 48 h with spherical aberration-corrected scanning transmission electron microscopy (Cs-STEM, Titan™ G^2 80-200 operated at 200 kV). HAADF images of the reacted nZVI particles (a and e); STEM-XEDS elemental mappings of Fe (Kα) (b and f), O (Kα) (c and g) and U (Lα) (d and h).

 This journal is © The Royal Society of Chemistry 2021

Published on 20 January 2021. Downloaded by Ege Universitesi on 6/12/2023 6:19:35 PM.

reactor size or reaction time, the dose of nZVI and recirculation ratio (Fig. 5). Specifically, the uranium removal efficiency increased from 85.44% to 99.34% as the nZVI dose increased from 1.97 to 9.85 g L^{-1} (Fig. 5a and Table S3†). When the HRT was decreased from 4 h to 1 h, there was no obvious decrease in the uranium removal efficiency (>99%). Nonetheless, as the volume of treated wastewater increased with shorter retention time, the breakthrough time (U < 5 μg L^{-1}) was much shorter (Fig. 5b). Thereby, only a relatively low HRT at 1 h is needed to achieve satisfactory uranium separation with an effluent concentration below 1 μg L^{-1}. As shown in Fig. 5c, the effluent uranium concentration increased to 4.5 μg L^{-1} at 39 h and remained at a quasi-steady state with only slight fluctuations till 60 h. The uranium concentration exceeded a breakthrough value of 5 μg L^{-1} within 8–10 h as R increased to 2.0 and 3.0. The removal efficiencies of uranium were 98.5%, 65.62% and 54.13%, respectively, for R = 1, 2, and 3.

Influence of the CSTR operational parameters on uranium enrichment and separation can be explained from the changes of physicochemical characteristics of nZVI. In the CSTR reactor, the co-existing species such as dissolved oxygen, nitrate and water reduce the reactivity of nZVI through the consumption of zero-valent iron, occupying surface sorption sites and changing the surface charge and solution pH (eqn (2) and (3)):

$$Fe^0 + 2H^+ \rightarrow Fe^{2+} + H_2 \quad (2)$$

$$Fe^0 + 2H_2O \rightarrow Fe^{2+} + 2OH^- + H_2\uparrow \quad (3)$$

At the nZVI dose of 1.97 g L^{-1}, the solution pH decreased from 8.91 to 6.33 and E_h increased from −0.53 to 0.27 V. However, the solution pH decreased from 8.80 to 8.51 and E_h increased from −0.49 to −0.18 V when the nZVI dose was 9.85 g L^{-1} (Fig. 5d and g). As a result, the equilibrium uranium

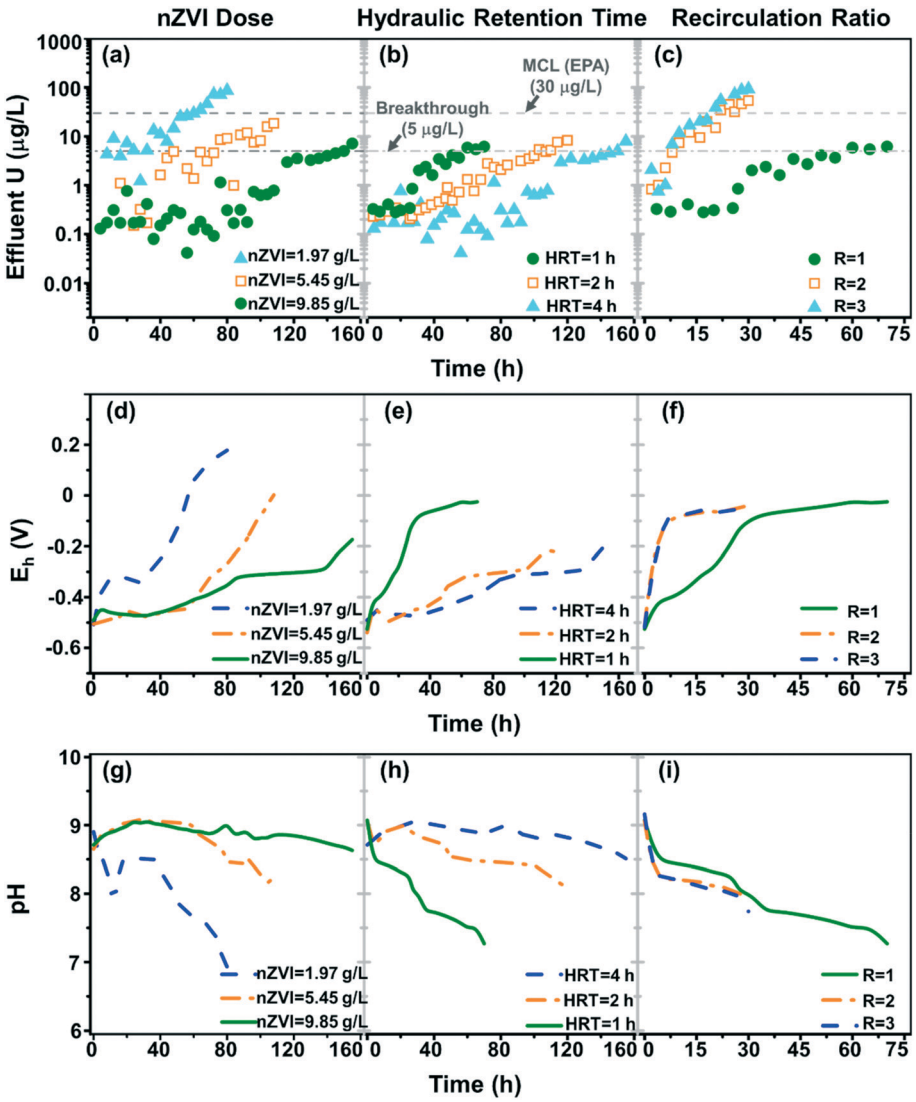


Fig. 5 Effects of the CSTR operational parameters on uranium enrichment: (a, d and g) nZVI dose, (b, e and h) hydraulic retention time (HRT) and (c, f and i) recirculation ratio (R).

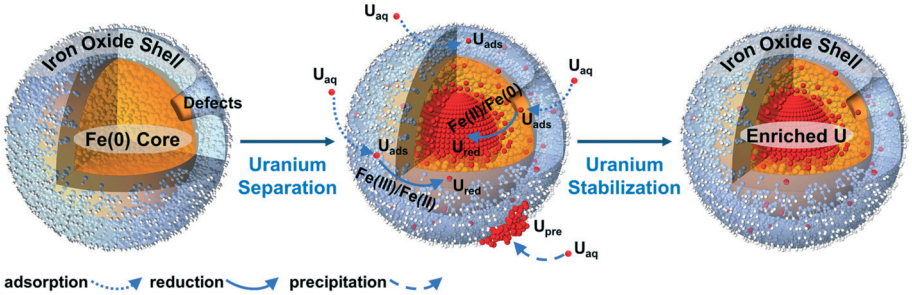


Fig. 6 Mechanisms for U(VI) removal with nZVI.[1,46,47]

Published on 20 January 2021. Downloaded by Ege Universitesi on 6/12/2023 6:19:35 PM.

phase at the end of the experiments changed from UO_2 to UO_2CO_3, which has a low affinity toward the nZVI surface, or to U_4O_9 as the nZVI dose increased from 1.97 g L^{-1} to 9.85 g L^{-1} nZVI. (Fig. S4a†). The evolution of solution E_h or pH was more dramatic as HRT decreased or recirculation ratio increased (Fig. 5). Under the predetermined HRT and R conditions, the stable uranium phases were in the reduced state (*e.g.*, UO_2 or U_4O_9) (Fig. S4b and S4c†).[37,38] And the deterioration of the effluent uranium concentration was caused by the insufficient reaction time between uranium and nZVI or settlement of nZVI particles in the clarifier tank (Fig. S5†).

3.5. Nanoencapsulation mechanisms

A conceptual model illustrating the reaction mechanisms of dissolved U(VI) with nZVI is presented in Fig. 6. Aqueous uranium ions are first attracted to nZVI *via* negatively charged surface $-OH^-$ groups and form surface complexes and then diffuse across the surface layer. The sorbed hexavalent uranium can readily accept electrons from the metallic iron and quickly reduced to lower valence states of U(IV):[39]

$$UO_2^{2+} + Fe^0 \rightarrow UO_{2(s)} + Fe^{2+} \quad (4)$$

$$UO_2^{2+} + 2Fe^{2+} \rightarrow UO_{2(s)} + 2Fe^{3+} \quad (5)$$

The equilibrium constants ($\log K$) for the above equations are 27.71 and 12.36 under standard conditions, which are several orders of magnitude higher than the adsorption constants ($\log K$ = −6.28–3.79).[40–44] The reduction of U(VI) to U(IV) (*e.g.*, UO_2) can thus be considered irreversible while the adsorption process has been proven reversible and highly dependent upon environmental conditions such as solution pH. In addition, U and other co-existing metal ions (*e.g.*, Al, Mn and Ca) can form (co)precipitates at high pH.[45] Ultimately, the adsorbed and/or reduced uranium deposits accumulate in the core zone of nZVI.[1] Theoretical mechanisms for uranium removal from aqueous solution by nZVI may include encapsulation, reduction, adsorption and precipitation.[1,2] Based upon the observed distribution of uranium within nZVI nanoparticles, solution and surface chemistry, the principal mechanisms are chemical reduction and intra-particle encapsulation.[1,46–48]

4. Conclusions

To evaluate the performance of nZVI remedying real uranium tailings wastewater with complex co-existing cations/anions, in this study, a novel uranium tailings wastewater treatment technology (*e.g.*, CSTR) was designed. The two-stage CSTR exhibited extremely high efficiencies for U and co-existing metal/metalloid ion (except Mn) removal. In the CSTR, 149.94 mg of uranium was recovered with only 0.12 g nZVI per L-wastewater and the average uranium concentration in the effluent was only 1.47 μg U per L which was more than one order of magnitude lower than that in the drinking water standard of USEPA (30 μg U per L). The content of uranium (wt%) in reacted iron oxides increased to 0.19%. The effects of operational parameters of CSTR for uranium enrichment and separation from radioactive wastewater (~311 μg U per L) and uranium removal mechanisms were investigated. Uranium removal efficiencies increased as nZVI dose increased or recirculation ratio decreased, and low hydraulic retention time (*e.g.*, 1 h) is beneficial to uranium separation processes. Results of the Cs-STEM, XRD, XPS, bicarbonate extraction analysis and theoretical calculations reveal that chemical reduction and intra-particle encapsulation are the principal uranium removal mechanisms. Compared with the previous reports of other groups, the wet chemistry and solids analysis results of this work demonstrated that the novel nZVI technology could be used to immobilize and enrich uranium from complex uranium-containing wastewater for a long period of time. This study may help to promote our understanding on the applications of nZVI to remedy radioactive wastewater and enrich valuable uranium resources.

Conflicts of interest

The authors declare that they have no known competing financial interests or personal relationships that could have appeared to influence the work reported in this paper.

This journal is © The Royal Society of Chemistry 2021

Published on 20 January 2021. Downloaded by Ege Universitesi on 6/12/2023 6:19:35 PM.

Acknowledgements

This work has been partially supported by the National Natural Science Foundation of China (NSFC Grants 41772243, 51978488 and 21277102), the Research Foundation of Education Bureau of Hunan Province, China (Grant No. 18C0432), the Natural Science Foundation of Hunan Province, China (Grant No. 2020JJ5489), and the China Post-doctoral Science Foundation (Grant No. 2018M642084).

References

1 L. Ling and W. X. Zhang, Enrichment and encapsulation of uranium with iron nanoparticle, *J. Am. Chem. Soc.*, 2015, **137**, 2788–2791.
2 S. Yan, B. Hua, Z. Y. Bao, J. Yang, C. X. Liu and B. L. Deng, Uranium(VI) removal by Nanoscale zerovalent iron in anoxic batch systems, *Environ. Sci. Technol.*, 2010, **44**, 7783–7789.
3 Y. L. Hua, W. Wang, X. Huang, T. Gu, D. Ding, L. Ling and W. X. Zhang, Effect of bicarbonate on aging and reactivity of nanoscale zerovalent iron (nZVI) toward uranium removal, *Chemosphere*, 2018, **201**, 603–611.
4 S. Tsarev, R. N. Collins, E. S. Ilton, A. Fahy and T. D. Waite, The short-term reduction of uranium by nanoscale zero-valent iron (nZVI): role of oxide shell, reduction mechanism and the formation of U(V)-carbonate phases, *Environ. Sci.: Nano*, 2017, **4**, 1304–1313.
5 H. Liu, M. Li, T. Chen, C. Chen, N. S. Alharbi, T. Hayat, D. Chen, Q. Zhang and Y. Sun, New synthesis of nZVI/C composites as an efficient adsorbent for the uptake of U(VI) from aqueous solutions, *Environ. Sci. Technol.*, 2017, **51**, 9227–9234.
6 A. Abdelouas, Uranium mill tailings: geochemistry, mineralogy, and environmental impact, *Elements*, 2006, **2**, 335–341.
7 C. Wang, Z. Baumann, D. J. Madigan and N. S. Fisher, Contaminated marine sediments as a source of cesium radioisotopes for benthic fauna near Fukushima, *Environ. Sci. Technol.*, 2016, **50**, 10448–10455.
8 S. C. Träber, V. Höllriegl, W. B. Li, U. Czeslik, W. Rühm, U. Oeh and B. Michalke, Estimating the absorption of soil-derived uranium in humans, *Environ. Sci. Technol.*, 2014, **48**, 14721–14727.
9 J. L. Anderson, R. D. Daniels, D. A. Fleming and C. Y. Tseng, Exposure assessment for a cohort of workers at a former uranium processing facility, *J. Exposure Sci. Environ. Epidemiol.*, 2012, **22**, 324–330.
10 I. G. Canu, S. Jacob, E. Cardis, P. Wild, S. Caer, A. Acker, M. Tirmarche and D. Laurier, Relationship between occupational exposure to uranium and cancer mortality, *Am. J. Epidemiol.*, 2010, **171**, S64–S64.
11 N. Casacuberta, M. Christl, K. O. Buesseler, Y. Lau, C. Vockenhuber, M. Castrillejo, H. A. Synal and P. Masque, Potential releases of 129I, 236U and Pu isotopes from the Fukushima Dai-ichi nuclear power plants to the ocean during 2013 to 2015, *Environ. Sci. Technol.*, 2017, **51**, 9826–9835.
12 G. Sheng, P. Yang, Y. Tang, Q. Hu, H. Li, X. Ren, B. Hu, X. Wang and Y. Huang, New insights into the primary roles of diatomite in the enhanced sequestration of UO2+ 2 by zerovalent iron nanoparticles: an advanced approach utilizing XPS and EXAFS, *Appl. Catal., B*, 2016, **193**, 189–197.
13 Y. Sun, C. Ding, W. Cheng and X. Wang, Simultaneous adsorption and reduction of U(VI) on reduced graphene oxide-supported nanoscale zerovalent iron, *J. Hazard. Mater.*, 2014, **280**, 399–408.
14 C. Jing, Y. Li, R. Cui and J. Xu, Illite-supported nanoscale zero-valent iron for removal of 238U from aqueous solution: characterization, reactivity and mechanism, *J. Radioanal. Nucl. Chem.*, 2015, **304**, 859–865.
15 G. D. Sheng, X. Y. Shao, Y. M. Li, J. F. Li, H. P. Dong, W. Cheng, X. Gao and Y. Y. Huang, Enhanced removal of uranium(VI) by nanoscale zerovalent iron supported on Na-bentonite and an investigation of mechanism, *J. Phys. Chem. A*, 2014, **118**, 2952–2958.
16 I. C. Popescu, P. Filip, D. Humelnicu, I. Humelnicu, T. B. Scott and R. A. Crane, Removal of uranium (VI) from aqueous systems by nanoscale zero-valent iron particles suspended in carboxy-methyl cellulose, *J. Nucl. Mater.*, 2013, **443**, 250–255.
17 S. Tsarev, R. N. Collins, A. Fahy and T. D. Waite, Reduced uranium phases produced from anaerobic reaction with nanoscale zerovalent iron, *Environ. Sci. Technol.*, 2016, **50**, 2595–2601.
18 O. Riba, T. B. Scott, K. V. Ragnarsdottir and G. C. Allen, Reaction mechanism of uranyl in the presence of zero-valent iron nanoparticles, *Geochim. Cosmochim. Acta*, 2008, **72**, 4047–4057.
19 S. Yan, Y. H. Chen, W. Xiang, Z. Y. Bao, C. X. Liu and B. L. Deng, Uranium(VI) reduction by nanoscale zero-valent iron in anoxic batch systems: the role of Fe(II) and Fe(III), *Chemosphere*, 2014, **117**, 625–630.
20 R. V. Davies, J. Kennedy, R. W. McIlroy, R. Spence and K. M. Hill, Extraction of uranium from sea water, *Nature*, 1964, **203**, 1110.
21 R. A. Crane, M. Dickinson, I. C. Popescu and T. B. Scott, Magnetite and zero-valent iron nanoparticles for the remediation of uranium contaminated environmental water, *Water Res.*, 2011, **45**, 2931–2942.
22 Y. P. Sun, X. Q. Li, J. Cao, W. X. Zhang and H. P. Wang, Characterization of zero-valent iron nanoparticles, *Adv. Colloid Interface Sci.*, 2006, **120**, 47–56.
23 L. Ling and W. X. Zhang, Visualizing arsenate reactions and encapsulation in a single zero-valent iron nanoparticle, *Environ. Sci. Technol.*, 2017, **51**, 2288–2294.
24 L. Ling, B. Pan and W. X. Zhang, Removal of selenium from water with nanoscale zero-valent iron: mechanisms of intraparticle reduction of Se(IV), *Water Res.*, 2015, **71**, 274–281.
25 A. R. Liu and W. X. Zhang, Fine structural features of nanoscale zero-valent iron characterized by spherical

Published on 20 January 2021. Downloaded by Ege Universitesi on 6/12/2023 6:19:35 PM.

aberration corrected scanning transmission electron microscopy (Cs-STEM), *Analyst*, 2014, **139**, 4512–4518.
26 F. M. Morel and J. G. Hering, *Principles and applications of aquatic chemistry*, Wiley-Interscience, New York, 1993.
27 L. Ling, X. Y. Huang, M. Li and W. X. Zhang, Mapping the reactions in a single zero-valent iron nanoparticle, *Environ. Sci. Technol.*, 2017, **51**, 14293–14300.
28 L. Ling and W. X. Zhang, Sequestration of Arsenate in Zero-Valent Iron Nanoparticles: Visualization of intraparticle reactions at angstrom resolution, *Environ. Sci. Technol. Lett.*, 2014, **1**, 305–309.
29 B. Gu, L. Liang, M. J. Dickey, X. Yin and S. Dai, Reductive Precipitation of uranium(VI) by zero-valent iron, *Environ. Sci. Technol.*, 1998, **32**, 3366–3373.
30 N. E. Agency and I. A. E. Agency, *Uranium 2016: resource, production and demand*, Organisation for Economic Co-operation and Development, Paris, 2016.
31 X. Q. Li and W. X. Zhang, Sequestration of metal cations with zerovalent iron nanoparticles - a study with high resolution X-ray photoelectron spectroscopy (HR-XPS), *J. Phys. Chem. C*, 2007, **111**, 6939–6946.
32 J. E. Martin, A. A. Herzing, W. Yan, X. Q. Li, B. E. Koel, C. J. Kiely and W. X. Zhang, Determination of the oxide layer thickness in core–shell zerovalent iron nanoparticles, *Langmuir*, 2008, **24**, 4329–4334.
33 Z. J. Li, L. Wang, L. Y. Yuan, C. L. Xiao, L. Mei, L. R. Zheng, J. Zhang, J. H. Yang, Y. L. Zhao, Z. T. Zhu, Z. F. Chai and W. Q. Shi, Efficient removal of uranium from aqueous solution by zero-valent iron nanoparticle and its graphene composite, *J. Hazard. Mater.*, 2015, **290**, 26–33.
34 L. N. Moyes, R. H. Parkman, J. M. Charnock, D. J. Vaughan, F. R. Livens, C. R. Hughes and A. Braithwaite, Uranium uptake from aqueous solution by interaction with goethite, lepidocrocite, muscovite, and mackinawite: An X-ray absorption spectroscopy study, *Environ. Sci. Technol.*, 2000, **34**, 1062–1068.
35 T. Hiemstra, W. H. Van Riemsdijk, A. Rossberg and K. U. Ulrich, A surface structural model for ferrihydrite II: adsorption of uranyl and carbonate, *Geochim. Cosmochim. Acta*, 2009, **73**, 4437–4451.
36 H. Zeng, A. Singh, S. Basak, K. U. Ulrich, M. Sahu, P. Biswas, J. G. Catalano and D. E. Giammar, Nanoscale size effects on uranium(VI) adsorption to hematite, *Environ. Sci. Technol.*, 2009, **43**, 1373–1378.
37 H. H. Huang, The Eh-pH diagram and its advances, *Metals*, 2016, **6**, 1–30.
38 G. Leinders, R. Bes, J. Pakarinen, K. Kvashnina and M. Verwerft, Evolution of the uranium chemical state in mixed-valence oxides, *Inorg. Chem.*, 2017, **56**, 6784–6787.
39 T. D. Waite, J. A. Davis, T. E. Payne, G. A. Waychunas and N. Xu, Uranium(VI) adsorption to ferrihydrite - application of a surface complexation model, *Geochim. Cosmochim. Acta*, 1994, **58**, 5465–5478.
40 M. O. Barnett, P. M. Jardine and S. C. Brooks, U(VI) Adsorption to heterogeneous subsurface media: application of a surface complexation model, *Environ. Sci. Technol.*, 2002, **36**, 937–942.
41 T. Cheng, M. O. Barnett, E. E. Roden and J. L. Zhuang, Effects of phosphate on uranium(VI) adsorption to goethite-coated sand, *Environ. Sci. Technol.*, 2004, **38**, 6059–6065.
42 C. Liu, J. M. Zachara, L. Zhong, R. Kukkadupa, J. E. Szecsody and D. W. Kennedy, Influence of sediment bioreduction and reoxidation on uranium sorption, *Environ. Sci. Technol.*, 2005, **39**, 4125–4133.
43 J. J. Mahoney, S. A. Cadle and R. T. Jakubowski, Uranyl adsorption onto hydrous ferric oxide—a re-evaluation for the diffuse layer model database, *Environ. Sci. Technol.*, 2009, **43**, 9260–9266.
44 I. Grenthe, J. Fuger, R. J. M. Konings, R. J. Lemire, A. B. Muller, C. N. T. Cregu and H. Wanner, *Chemical thermodynamics of uranium*, France, Paris, 2004.
45 M. I. Nystrand, P. Osterholm, C. X. Yu and M. Astrom, Distribution and speciation of metals, phosphorus, sulfate and organic material in brackish estuary water affected by acid sulfate soils, *Appl. Geochem.*, 2016, **66**, 264–274.
46 L. Ling, X. Y. Huang and W. X. Zhang, Enrichment of precious metals from wastewater with core-shell nanoparticles of iron, *Adv. Mater.*, 2018, **30**(17), e1705703.
47 X. Y. Huang, L. Ling and W. X. Zhang, Nanoencapsulation of hexavalent chromium with nanoscale zero-valent iron: High resolution chemical mapping of the passivation layer, *J. Environ. Sci.*, 2018, **67**, 4–13.
48 H. M. Zhang, Y. Ruan, A. P. Liang, K. M. Shih, Z. H. Diao, M. H. Su, L. A. Hou, D. Y. Chen, H. Lu and L. J. Kong, Carbothermal reduction for preparing nZVI/BC to extract uranium: Insight into the iron species dependent uranium adsorption behavior, *J. Cleaner Prod.*, 2019, **239**, 1–9.

 This journal is © The Royal Society of Chemistry 2021